

DESY 80/22
March 1980



HEAD TAIL TURBULENCE AND THE TRANSVERSE PETRA INSTABILITY

by

R. D. Kohaupt

To be sure that your preprints are promptly included in the
HIGH ENERGY PHYSICS INDEX ,
send them to the following address (if possible by air mail) :

**DESY
Bibliothek
Notkestrasse 85
2 Hamburg 52
Germany**

Introduction

In this article a transverse instability mechanism is described which seems to agree with the observations of a vertical instability limiting the single bunch currents in PETRA^(1,2)

Except for the head-tail instability of betatron oscillations, driven by the chromaticity dependent phase shift between head and tail collectives, a single bunch is transversely stable in the case of short range forces.^(*)

HEAD TAIL TURBULENCE AND THE TRANSVERSE

PETRA INSTABILITY

As was pointed out by F. Sacherer⁽³⁾ for the longitudinal motion, this "stability" is due to the fact that a single bunch mode is a "standing wave" pattern combined of two travelling waves travelling in opposite directions. Since one of the waves is unstable the other, however, is stable, the standing wave combination has indifferent stability.

R.D. Kohaupt

Although the recombination of an unstable travelling wave is destroyed by phase oscillations, an instability can occur if the growth rate of the unstable wave exceeds the synchrotron frequency. This mechanism is the physical base of the coasting beam model of longitudinal turbulence^(4,5).

Contents

Introduction

Section I

1. Equations of motion
2. Vlasov equation
3. Currents and forces
4. Integral equation and threshold

Section II

1. Observations at PETRA
2. Model properties
3. Quantitative estimates and scaling laws
4. Conclusion

In analogy to the longitudinal turbulence also for the transverse head-tail motion unstable travelling waves can be recombined from head-tail standing wave patterns by head-tail mode coupling. For sufficiently high single bunch intensities this mechanism leads to an instability which occurs even if the chromaticity is zero.

In section I of this article the theoretical analysis is presented while in section II the consequences of the model with respect to PETRA observations are discussed.

(*) The small "Robinson-effect" can be neglected.

Section I

1. Equations of motion

For the description of the transverse and longitudinal motion we introduce the transverse coordinate x and the azimuth φ . We define

$$Z = \frac{x}{\sqrt{\beta}}, \quad \tau = \frac{y(s)}{\omega} \quad (1)$$

$\beta, y(s), \omega$ being the amplitude function, the phase advance and the betatron frequency. The longitudinal coordinate φ will be parameterized according to synchrotron oscillations.

$$\dot{\varphi} = \tau \cos \varphi, \quad \dot{\tau} = -\omega_s \tau \sin \varphi \quad (2)$$

where ω_s denotes the synchrotron frequency.

In terms of the "quasi-time" τ the equations for the transverse motion read (6,7)

$$\ddot{y} = -\frac{dZ}{d\tau}, \quad \frac{d^2 y}{d\tau^2} = -\omega^2 Z + \frac{F}{E} \omega^2 \beta^{3/2} \quad (3)$$

Here F denotes the force generated by collective interaction. Changing to the coordinates Q and q of betatron motion yields:

$$\begin{aligned} Z &= q \cos y, \\ \frac{dy}{d\tau} &= \omega_\beta + \frac{y}{\alpha} \omega_s \tau \sin \varphi, \\ \frac{d\tau}{d\tau} &= -\omega_\beta \frac{F}{E} \beta^{3/2} \sin \varphi \end{aligned} \quad \begin{matrix} (*) \\ (**) \end{matrix}$$

(*) We neglect the betatron phase shift within the bunch

(**) We neglect terms of the order $F \frac{y}{\alpha} \tau$

ξ, α being chromaticity and momentum compaction factor, and ω_β denotes the free betatron frequency for $\xi = 0$

2. Vlasov equation

In the following chapters we apply the Sacherer formalism. According to perturbation theory we write the particle density function in the form:

$$W = f + W_0(\tau) u_0(s), \quad (5)$$

where $W_0(\tau) u_0(s)$ is the stationary distribution, and f describes the perturbation.

The linearized Vlasov equation then follows from (4) and (5)

$$\left\{ \frac{\partial}{\partial \tau} + \left[\omega_\beta + \frac{y}{\alpha} \omega_s \tau \sin \varphi \right] \frac{\partial}{\partial y} + \omega_s \frac{\partial}{\partial \varphi} \right\} f = \frac{F[f]}{E} \omega_\beta^{3/2} \omega_0(\tau) \frac{\partial u_0(s)}{\partial s} \sin y \quad (6)$$

Here we have explicitly written F as a linear functional of f . Neglecting terms of the order $F \times \frac{y}{\alpha} \tau$, equ. (6) can be solved by a density function of the form:

$$f = f_\beta(s, y) g(\tau, \varphi) e^{i \frac{y}{\alpha} \tau - i \Omega \tau} \quad (7)$$

Because of (4) we define the amplitude of the dipole moment as

$$\bar{Z} = \int_{-\pi}^{+\pi} dy \int_0^{2\pi} ds f_\beta(s, y) \cos y \quad (8)$$

Following equ. (7) we write

$$f = \sum_m \alpha_m e^{im\varphi} e^{i \frac{y}{\alpha} \tau} \left\{ \cos y + i \frac{\Omega - m \omega_s}{\omega_\beta} \sin y \right\} e^{-i \Omega \tau} \quad (9)$$

(*) We neglect the difference between t and τ for the synchrotron oscillation.

Inserting (9) into (6) we obtain in first approximation:

$$a_m = \frac{-\omega_p}{\omega_p^2 - (\Omega - m\omega_c)^2} \int_{-\pi}^{\pi} d\psi e^{-im\psi - i\frac{\omega_c}{2} \psi} e^{i\frac{\omega_c}{2} \psi} \frac{F}{E} \beta^{3/2} \omega_0(r) \frac{\partial U_0(q)}{\partial q} \quad (10)$$

Defining

$$g(r, \psi) = \sum_m g_m(r) e^{im\psi} \quad (11)$$

$$g(\vartheta) = \int d\psi d\tau g(r, \psi) \delta(\vartheta - \tau \omega_0 \psi)$$

and using (8), we find

$$g_m(r) \bar{z} = \frac{\omega_p^2}{\omega_p^2 - (\Omega - m\omega_c)^2} \int_{-\pi}^{\pi} d\psi e^{-im\psi - i\frac{\omega_c}{2} \psi} e^{i\frac{\omega_c}{2} \psi} \frac{F}{E} \beta^{3/2} \omega_0(r) \quad (12)$$

3. Currents and forces

In agreement with (7) the head-tail motion of a bunch can be described by the dipole mode function.

$$d(\tau) = \bar{x} g(\vartheta) e^{-i\frac{\omega_c}{2} \vartheta} e^{i\frac{\omega_c}{2} \vartheta} \quad (13)$$

The bunch circulates with revolution frequency $\frac{\omega_0}{2\pi}$, so that at a local place because of

$$\omega_0 t = 2\pi \nu - \vartheta$$

the bunch produces a time dependent signal proportional to the dipole moment times average current \bar{J} :

$$S(t) = \bar{J} \sum_p \tilde{g}(p - \frac{1}{2}) e^{-i\omega_0 t} e^{-i\Omega t} \bar{x} \quad (14)$$

with

$$\tilde{g}(q) = \int_{-\pi}^{\pi} d\vartheta g(\vartheta) e^{-iq\vartheta}$$

At this step we make the assumption that the amplitude function within an object in the ring, driving the instability, is nearly constant, so that

$$\tilde{g} \approx \frac{t}{\eta} \quad (15)$$

Thus from (13) follows

$$S(t) = \bar{J} \sum_p e^{-i\Omega t} \tilde{g}(p - \frac{1}{2}) e^{-ip\omega_0 t} \bar{x} \quad (16)$$

The signal (15) generates transversely acting fields in such objects of the form:

$$A_\mu = \bar{J} \sum_p \bar{A}_\mu(p + \frac{q_p}{2}) \tilde{g}(p - \frac{1}{2}) e^{-ip\omega_0 t} e^{-i\Omega t} \bar{x}; \quad \mu = 0, \dots, 3 \quad (17)$$

where $\bar{A}_\mu(q)$ is the response function of the local object. According to first order theory we have replaced Ω by $\omega_p = Q\beta\omega_0$, so that the local Q -value appears in the response function as was expected for short range fields.

The bunch center arrives at the local object at $t_0 = \frac{2\pi\gamma}{\omega_0} - \nu\tau$, and the forces acting within the bunch can be written as:

$$F = \bar{J} \sum_p G(t, p + \frac{q_p}{2}) \tilde{g}(p - \frac{1}{2}) e^{-ip\vartheta} e^{-i\Omega t} \bar{x} \quad (18)$$

The time dependence of G accounts for the fact that the forces at the position ϑ act only during the time of passage. The function $G(t, q)$ is periodic in t with the periode τ , and because of the definition (1) of τ , G is also periodic in τ with τ :

$$G(t[\tau], q) = \sum_k G_k(q) e^{ik\omega_0 \tau} \quad (19)$$

The forces F excite betatron oscillations essentially only around $\Omega \approx \omega_p$. Accounting for the extra factor $e^{-i\Omega t}$ in (17), we have only to retain G_0 in this equation:

$$G_0(q) = \frac{1}{\tau} \int d\tau G(t[\tau], q) = \frac{1}{\tau(s_0)} \frac{1}{\tau} \int dt G(t, q) \quad (20)$$

with

$$\tau(s_0) = \beta(s_0) / Q\beta$$

where R denotes the main radius of the machine and S_0 the position of the object. Starting from (17), (19) we can make use of the standard definition of the transverse impedance $\{9, 10\}$ to rewrite the forces acting on the bunch:

$$F[\vartheta] = \frac{1}{\tau} \frac{e}{2\pi R} \bar{x} \sum_p Z_\perp(p) \tilde{g}(p - \frac{1}{2}) e^{-ip\vartheta} e^{-i\Omega t}$$

Here we have dropped the $\frac{Q}{2}$ -dependence for a "broad band" impedance Z_{\perp} .

4. Integral equation and threshold

Going back to (11) yields:

$$\left[\frac{\Omega - (\omega_{\beta} + m\omega_s)}{2} \omega_0(\tau) \sum_p Z_{\perp}(p) \int_{-i}^m \tilde{g}_m(p) \tilde{g}_m(\rho - \frac{\rho - \xi}{\alpha}) \tilde{g}(\rho - \frac{\rho - \xi}{\alpha}) \right] g_m(\tau) \approx \tag{21}$$

The function $\tilde{g}(q)$ are related to the $g_m(x)$ by

$$\tilde{g}(q) = 2\pi \sum_m [-i]^m \int d\tau' g_m(\tau') \tilde{g}_m(q\tau') \tag{22}$$

Then from (21), (22) and with the abbreviation

$$\Omega - (\omega_{\beta} + m\omega_s) = \lambda_m \tag{23}$$

the integral equation for $g_m(x)$ follows:

$$\lambda_m g_m(\tau) = \frac{\sqrt{\beta^3} \omega_{\beta}}{4\pi R E / e \eta} \omega_0(\tau) \times 2\pi \times \times \sum_n \int d\tau' g_n(\tau') \int_{-i}^{m-n-1} \sum_p Z_{\perp}(p) \int_m^{\rho - \frac{\rho - \xi}{\alpha}} \tilde{g}_m(\rho - \frac{\rho - \xi}{\alpha}) \tilde{g}(\rho - \frac{\rho - \xi}{\alpha}) \tag{24}$$

We now proceed to rewrite (24) in a more convenient form.

Following Sacherer (8) we introduce the adjoint functions

$$\omega_0^{\dagger}(\tau) \tilde{g}^{\dagger} = g \tag{25}$$

and the scalar product

$$(g_m^{\dagger}, g_n) = \int d\tau' g_m^{\dagger}(\tau') g_n(\tau) \tag{26}$$

Further we write the solutions of (24) in the form :

$$g_m(\tau) = A_m l_m(\tau) \tag{27}$$

with $(l_m^{\dagger}, l_m) = 1$

Finally we introduce

$$h_m(q) = \sqrt{2\pi} \int d\tau' \tilde{g}_m(q\tau) l_m(\tau) \tag{29}$$

From (24) then we obtain the final equations:

$$\lambda_m A_m = \sum_n M_{mn}(\xi) A_n$$

$$M_{mn} = \frac{\sqrt{\beta^3} \omega_{\beta}}{4\pi R E / e} \int_{-i}^{m-n-1} \sum_p Z_{\perp}(p) h_m(\rho - \frac{\rho - \xi}{\alpha}) h_n(\rho - \frac{\rho - \xi}{\alpha}) \tag{30}$$

In equ. (30) the different head-tail modes are coupled. For $\xi = 0$ the frequencies of different modes m, m' are different:

$$\Omega_m - \Omega_{m'} = (m - m') \omega_s \tag{31}$$

For weak interactions, where the absolute value of the frequency shift is small as compared to the synchrotron frequency, all terms with $n \neq m$ on the r.h.s. of equation (30) can be dropped. Because of the reflection property of Z_{\perp}

$$Z_{\perp}(p) = -Z_{\perp}^{\dagger}(-p) \tag{32}$$

the imaginary part of $M_{mn}(\xi)$ causing instability vanishes except for $\xi \neq 0$. This behaviour describes the "conventional" head-tail instability. (10, 11)

For high intensities, however, mode coupling can become important. We consider two modes

$$m = 1 \text{ (odd)}, m = 2 \text{ (even)}$$

with

$$\Omega_2 - \Omega_{-1} = \omega_s$$

for $I = 0$.

At high intensities the frequency shift may exceed ω_s , so that we have to retain mode $m=1$ and $m=2$. From (30) we obtain the symmetry properties of M_{mn}

$$M_{21} = -M_{12} \quad (33)$$

and for even-odd mode-coupling (30) leads to

$$\begin{vmatrix} \lambda - M_{11}(\xi) & M_{12}(\xi) \\ -M_{12}(\xi) & \lambda - \omega_s - M_{22}(\xi) \end{vmatrix} = 0 \quad (34)$$

Because of the reflection properties of the Bessel functions $I_m(\eta)$ the functions h_m satisfy

$$h_m(p) = (-1)^m h_m(-p) \quad (35)$$

From (32) and (35) then follows, that the real part of $M_{12}(\xi)$ does not vanish even for $\xi = 0$. For $\xi = 0$ we obtain from (35)

$$\lambda = \frac{1}{2} \left\{ \omega_s \pm \sqrt{\omega_s^2 - 4M_{12}^2} \right\} \quad (36)$$

and a "travelling wave instability" occurs if

$$|M_{12}| > \frac{\omega_s}{2} \quad (37)$$

We introduce $\Delta M(\xi)$ defined by

$$\Delta M(\xi) = M_{22}(\xi) - M_{11}(\xi) \quad (38)$$

and obtain λ as a function of the chromaticity:

$$\lambda = \frac{1}{2} (M_{11}(\xi) + M_{22}(\xi)) + \frac{1}{2} (\omega_s \pm \sqrt{(\omega_s + \Delta M(\xi))^2 - 4M_{12}^2(\xi)}) \quad (39)$$

In the next section (section II) the complex frequency shift (39) will be studied with respect to the observations concerning the vertical instability in FERPA.

Section II

1. Observations at FERPA

We start with a review of observations concerning the transverse instability in FERPA (1,2):

1. Observation:
The instability occurs vertically.

2. Observation:
The instability is a single bunch instability. No signals are observed confirming a center of mass motion.

3. Observation:
The instability occurs even for $\xi = 0$, and the strength of the instability increases with increasing ξ .

4. Observation:
The instability increases with increasing higher order mode losses.

5. Observation:
When the vertical Landau damping is increased changing the horizontal beam size, the threshold current remains nearly constant.

2. Model properties

1. Property:
From equation (30) we find that the elements M_{mn} are proportional to the amplitude function.
In FERPA one has in the rf cavity sections:

$$\beta_{\text{vert.}} \approx \beta_{\text{hor.}}$$

so that the vertical instability occurs first.

2. PROPERTY

We consider Fig.1 and assume that the p-dependence of $\partial_L Z_L$ has the form shown by the dashed line. Starting with the low frequency resistive wall part (a) which mainly drives the fundamental head-tail instability, a flat minimum (b) follows, so that the head-tail mode coupling between $m = 0$ and $m = 1$ characterized by the overlap region of h_0, h_1 (shaded area) does not exceed the travelling wave threshold.

Therefore no center of mass motion is excited. After a "gentle" slope which stabilizes the head-tail mode $m = 1$ for $\zeta > 0$ ($\text{Im } M_{11} < 0$), the impedance reaches a flat maximum (c) in the overlap area of h_1, h_2 . This maximum drives the travelling wave instability due to the coupling of the modes $m = 1, m = 2$. After passing the maximum, the impedance decreases leading to an unstable head-tail mode $m = 2$ for $\zeta > 0$ ($\text{Im } M_{12} > 0$). Because of these properties of M_{11}, M_{22} , we drop the first term on the r.h.s. of equ. (39)

From the definition (36) of ΔM we obtain:
 $\text{Lim } \Delta M_1 = |\text{Im } M_{12}| + |\text{Im } M_{11}|$,
 so that the instability threshold is reduced for $\zeta > 0$ in agreement with the observation.

4. PROPERTY:

The transverse impedance is directly related to the higher order mode loss impedance

5. PROPERTY:

For simplicity we put $\zeta = 0$ in equ. (30). The threshold current is then defined by

$$\delta_R + \delta_L = \frac{1}{2} \sqrt{4M_{12}^2(\bar{J}) - \omega_3^2} \quad (40)$$

where δ_R, δ_L denote radiation and Landau-damping. Resolving for $M_{12}(\bar{J})$ yields

$$M_{12}(\bar{J}) = \frac{1}{2} \sqrt{4(\delta_R + \delta_L)^2 + \omega_3^2} \quad (41)$$

Since $\delta_R, \delta_L \ll \omega_3$ in PETRA, the threshold current is nearly independent of δ_L (and δ_R).

3. Quantitative estimates and scaling laws

In order to get a quantitative estimate of the instability strength, we relate $\partial_L Z_L = R_L$ to the longitudinal resistive impedance $R_{||}$ causing the higher order mode losses (10)

$$R_L \approx \frac{2c R_{||}}{b^2 \omega_0 p}$$

where b denotes the effective radius of the localized cavity-like object in the ring.

The sum over p on the r.h.s. of equ. (30) is substituted very roughly according to:

$$\sum_p Z_L(p) h_m h_n \rightarrow \frac{2c}{b^2 \omega_0 R} \frac{\sigma}{Z_{\text{eff}}^{(HOML)}} 2\sigma \triangleq \text{bunchlength} \quad (42)$$

Here $Z_{\text{eff}}^{(HOML)}$ is the effective higher mode loss impedance. We obtain from equ. (30):

$$M_{12} \approx \frac{1}{2\pi} \frac{\sigma}{\epsilon_b} R \frac{\beta}{b} \frac{J Z_{\text{eff}}^{(HOML)}}{E/e}; \quad \epsilon_b = \frac{b}{c} \quad (43)$$

Passing to numerical values yields:

a) PETRA

$$\begin{aligned} \omega_3/2 &\approx 24 \text{ kHz} \\ b &\approx 5 \text{ cm} \\ \frac{\sigma}{2\pi R} &\approx 10^{-5} \implies M_{12} \approx 20 \text{ kHz} \\ \beta &\approx 25 \text{ m} \\ E &= 6 \text{ GeV} \\ J Z_{\text{eff}}^{(HOML)} &\approx 4 \cdot 10^6 \text{ V at } 10 \text{ mA} \end{aligned}$$

Together with equ. (41) the head-tail mode coupling seems to be possible in PETRA.

(*) For the extra factor $\frac{\sigma}{R}$ on the r.h.s. of equ. (42) see ref. (12)

b. DORIS

$$\begin{aligned}
 \omega_s/2 &\approx 120 \text{ kHz} \\
 b &\approx 5 \text{ cm} \\
 \frac{\sigma}{2\pi R} &\approx 9 \cdot 10^{-4} \implies M_{12} \approx 72 \text{ kHz} \\
 \beta &\approx 20 \text{ m} \\
 E &= 4 \text{ GeV} \\
 \bar{J} Z_{\text{eff}}^{(HOML)} &\approx 4 \cdot 10^5 \text{ V at } 50 \text{ mA}
 \end{aligned}$$

Although the single bunch currents in DORIS at 4 GeV are sometimes limited by a vertical instability above 50 mA, there is no significant observation which supports the head-tail turbulence model.

Starting from equs (41) and (43) we derive a general scaling law:

$$\frac{1}{\sigma_b} \frac{\beta}{b} \frac{\bar{J} Z_{\text{eff}}^{(HOML)}}{E/c} \frac{\sigma}{R} \sim \omega_s \quad (45)$$

In addition to (45) we introduce the following general scaling laws:

$$\begin{aligned}
 \sigma &\sim \frac{1}{Q_s} (\bar{J} Z_0)^2 E^{\alpha c} \\
 Z_{\text{eff}}^{(HOML)} &\sim Z_0 \frac{R}{\sigma \cdot \beta} \\
 Q_s &= \frac{\omega_s}{\omega_0} \quad (46)
 \end{aligned}$$

where $\mu_s, \beta, \alpha c$ are powers to be determined either by theory

(*) Z_0 is proportional to the longitudinal impedance of the driving objects.

or experiment. From (45) and (46) we find a scaling law for \bar{J} :

$$\bar{J} \sim \left(\frac{b}{\beta} \right)^{\frac{1}{\alpha c}} \frac{1 + \alpha c (h-1)}{\gamma^{1-\alpha c} (h-1)} Q_s^{\frac{1-\alpha c (h-1)}{\alpha c}} \frac{1}{Z_0} \quad (47)$$

In particular PETRA experiments (2,13) we observed $Q_s \approx 0.5, \alpha c \approx 0, \beta \approx 1.5$. These numbers lead to

$$\bar{J} \sim \left(\frac{1}{\beta} \right)^{4/3} \gamma^{4/3}$$

The observed threshold currents are in good agreement with the $\left(\frac{1}{\beta} \right)^{4/3}$ - dependence.

Going from 6 GeV to 7 GeV also the $\gamma^{4/3}$ -dependence is established. Going from 6 GeV to 5 GeV the current decreases like γ^3 . It should be remarked, however, that the vertical blow up at 5 GeV was not safely identified as the vertical PETRA instability. In earlier experiments the threshold current behaved as γ .

Conclusions

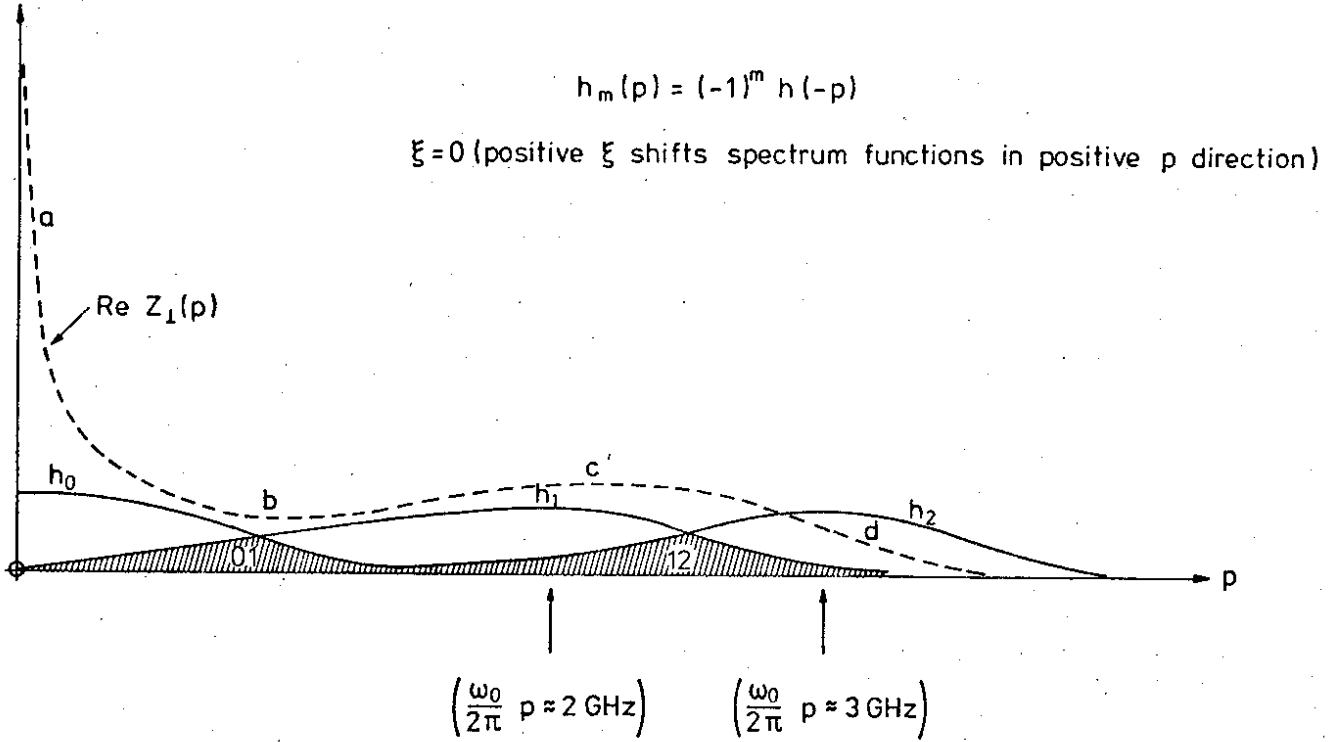
The head-tail turbulence could be further established if coupled head-tail modes were observed. In PETRA this was tried applying optical methods. There is an indication of internal betatron oscillations of the bunch, however, we have to continue these first experiments until the experimental methods are clearly understood.

Since the model predicts a higher threshold of the instability if Q_s is sufficiently high, the Q_s -dependence of the PETRA instability has to be carefully investigated in future machine experiments. (*)

The formalism applied in this article can be extended also to betatron quadrupole oscillations. Work along this line is in progress.

(*) Recent observations show that the single bunch current increases with increasing Q_s .

Re $Z_{\perp}(p)$, $h_m(p)$



Assumed real part of transverse impedance as a function of the multiple p of revolution frequency

Fig. 1

References

1. R.D.Kohaupt, 1979 Particle Accelerator Conference, P.3480 (1979)
2. R.D.Kohaupt, PETRA, Vorl. Bericht, (1979)
3. F. Sacherer, CERN/PS/BR/77-5, (1977)
4. M. Korth, E.Messerschmid, BNL 22411, (1977)
5. A.W.Chao, I.Carey, PEP 224, (1977)
6. E.J.Courant, H.S.Snyder, Annals of Physics 3, (1958)
7. R.D.Kohaupt, DESY H1-74/2 (1974)
8. F.Sacherer, CERN/SI-BR/72-5 (1972)
9. See ref. 10
10. F.Sacherer, MFS/Int.BR/74-8 (1974)
11. A.W.Chao, C.Y. Yao, PEP Note-321, (1979)
12. F.Sacherer, PEP Note-45, (1973)
13. C.J.Voss et al., DESY 80/10, (1980) (to be published)